

Experimental-Numerical Analysis of a Flat Plate Subjected to Shearing and Manufactured by Incremental Techniques

Tomasz Kopecki^{1*}, Łukasz Świąch¹

¹ Department of Aviation and Mechanical Engineering, Rzeszów University of Technology, Aleja Powstańców Warszawy 8, 35-029 Rzeszów, Poland

* Corresponding author's e-mail: tkopecki@prz.edu.pl

ABSTRACT

The paper presents the results of experimental studies and numerical analyses using the Finite Elements Method for a planar structure subjected to pure shear. The test specimen was made using an Fused Filament Fabrication incremental technique. In order to correctly represent the mechanical properties of the structure, a series of tests were performed to determine the physical constants of the model material used. Due to the perfect physical nature of the numerical model, in contrast to experimental phenomena, a suitable method was employed to induce the post-critical deformations in the analysed structure.

Keywords: 3D printing, advanced deformation, finite elements method, nonlinear analysis, composite.

INTRODUCTION

Manufacturing techniques based on 3D printing are increasingly important in many modern technology sectors. As the efficiency of materials engineering has increased significantly in creating new materials for use in this type of technology, and as the capabilities of the printing devices themselves have increased, the mechanical properties of printed components are less and less different from those of components manufactured by traditional techniques such as machining [11]. Particularly in the aerospace and automotive industries, the use of the latter often requires several complex operations where raw materials are relatively inefficient (large amounts of waste, which are not directly suitable for further use). Moreover, this machining is only possible with materials of sufficiently low hardness, which often leads to additional heat treatment, for instance in the case of steel components.

Other manufacturing techniques also generally require the use of complex, multi-stage processes. Unlike those mentioned above, incremental printing techniques are usually based on closed

one-step processes due to their nature [7, 14]. In the case of metal structures, using a laser offers the possibility to carry out proper heat treatment of the raw material. This results in a finished structural element with the required mechanical properties. In addition, one of the main advantages of incremental techniques is that the raw material used is practically not wasted.

A promising prospect for the aerospace sector is the possibility of using printed structures made from special materials, such as carbon fibre-reinforced polymers, which could be a practical alternative to the fibre composites used today.

In polymeric raw material printing techniques, the process involves sequentially dispensing liquid material through a nozzle of a certain diameter [19, 20]. As a result, the structure of the printed component is characterised by a lack of perfect homogeneity and cannot be considered isotropic. As detailed observations of one of the compressed layers show, its cross-sectional geometry is such that it can weaken the load-bearing capacity of the structure under some kinds of loads (Fig. 1).

Since the mechanical properties of a single printed layer are orthotropic, it seems appropriate



Figure 1. Geometric form of a cross-section of a single printed layer

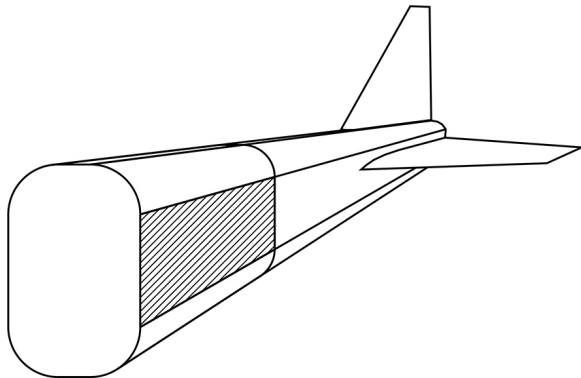


Figure 2. An example of a flat surface within a working covering of a semi-shell hull structure

for numerical applications to treat this type of structure as a layered composite. Most printing devices can precisely define the orientation of individual layers so that, for example, successive layers can be printed at right angles to each other. The numerical model can then be based on a typical layered composite structure. However, to perform a numerical analysis, laboratory tests are needed to determine the physical constants of the printed structure.

Although incremental techniques allow the free formation of spatial structures, among the load-bearing structures used in aviation, flat or near-flat structures with a very low curvature with respect to the surface and usually with a shear function play an important role. These include, for example, wing spar walls or parts of the working wing and fuselage coverings (Fig. 2).

Therefore, it seems appropriate to conduct experimental research, develop numerical models of such printed structures, and develop new solutions to increase their strength and reduce their susceptibility to post-critical deformations [1][3]. Improvements in numerical modelling methods are also warranted, in particular ways of mapping post-critical deformations [12].

PURPOSE AND SCOPE OF THE STUDY

The object of consideration was the plate made using 3D printing, subjected to pure shear (Fig. 3). The thickness of the model was 2 mm and the test area had dimensions of 172 mm ×

172 mm. For the experimental testing, a separate testing device was used, running on a Zwick Roell Z050 universal testing machine. The analyses aimed to determine the type and magnitude of the post-critical deformations of the object and develop techniques to implement an adequate numerical model whose results would satisfactorily match the experimental results.

The model was made from the popular, biodegradable polymer PLA (polylactide acid). It is a material with favourable mechanical properties from the point of view of model testing, with a fairly significant elastic range.

The process of 3D printing of the model was carried out using of the ULTIMAKER S5 printer, with closed printing space, providing the temperature rigor. The used filament was produced and recommended by the producer of the printer. The printing head was equipped with the extruder of 0.4 mm diameter. The range of used printing

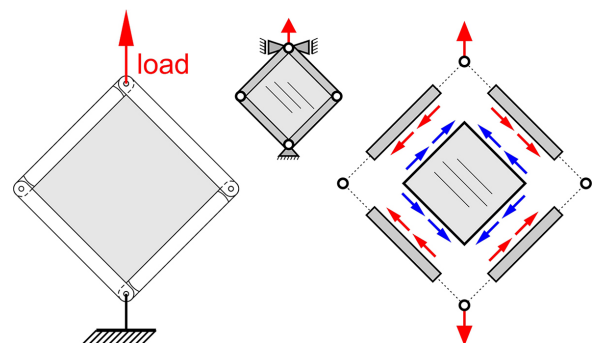


Figure 3. Scheme of the structure under consideration

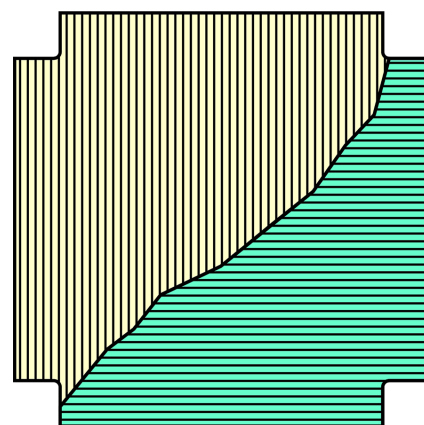


Figure 4. Orientation diagram for successive layers of spatial print

temperatures of PLA filament was 205–225 °C. Air circulation inside the printing head was provided by means of fan system.

The spatial print layers of the experimental model were 0.1 mm thick. The print fibres were orientated alternately at angles of 0/90 degrees to the main directions (Fig. 4). The model was carried out using 100% infill parameter.

Because of the way it is made, the analysed structure cannot be regarded as an isotropic material. The manner in which the individual layers are applied allows an assumption to be made about their orthotropic characteristics. Thus, the structure under study can be considered as a kind of sandwich composite, and its numerical model should be based on this assumption [8, 9].

Although the chemical composition of PLA filaments is theoretically the same regardless of the manufacturer, their specific production conditions and the addition of impurities such as dyes cause significant differences in their mechanical properties. In addition, the physical characteristics of the printed structure itself are also greatly influenced by the printing process and its parameters. Therefore, the correct determination of the physical constants of the structure material requires an appropriate experiment.

The derivation of the numerical model was preceded by a series of tests on samples prepared in stages using the same printing parameters as in the experimental plate model. The tests were performed on a Zwick Roell Z030 testing machine

equipped with an extensometer to accurately measure the longitudinal and transverse growth of the sample (Fig. 5).

Numerical analyses were performed using the MSC PATRAN/MARC software, which is characterised by a considerable capability for user-defined parameters of nonlinear procedures and a wide range of these procedures, allowing efficient reproduction of geometric nonlinearities.

Due to the two-dimensional nature of the load system, transitions had to be started perpendicular to the plane of the model in order to correctly represent the post-critical deformations. A method extensively described in an earlier publication by one of the authors [10] was used.

EXPERIMENTAL RESEARCH

The main test was carried out with a specific load system, which is a mechanism to fix and apply a load to the structure under test (Fig. 6). The model was fixed using bolted connections.

The loading system worked with a universal testing machine, with which the load value was controlled. Deformation measurements of the model were carried out using a GOM ARAMIS optical scanner.

The experiment resulted in a visualisation of the model displacements and representative equilibrium paths showing the relationship between load and displacements at selected points (Fig. 7–8).



Figure 5. Testing machine equipped with biaxial extensometer

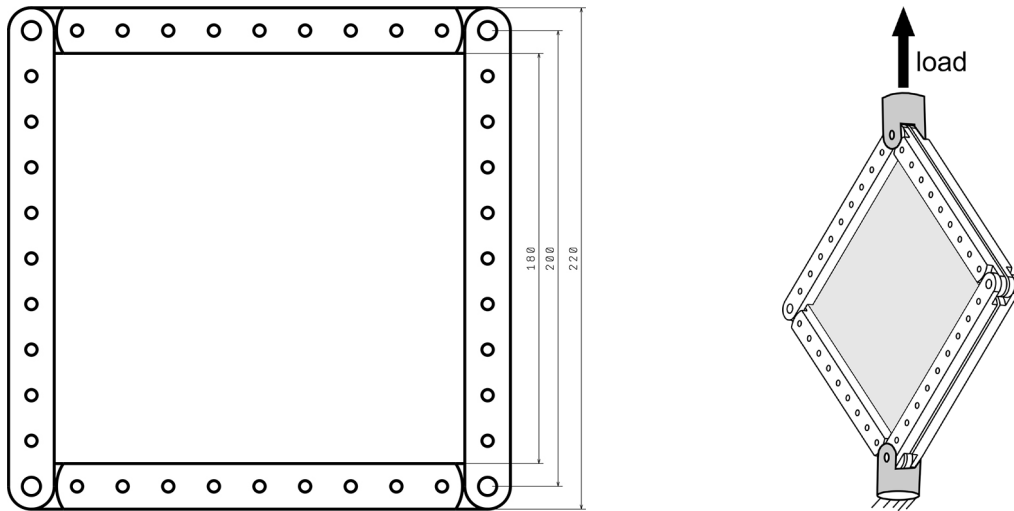


Figure 6. Dimensions and working principle of the loading system

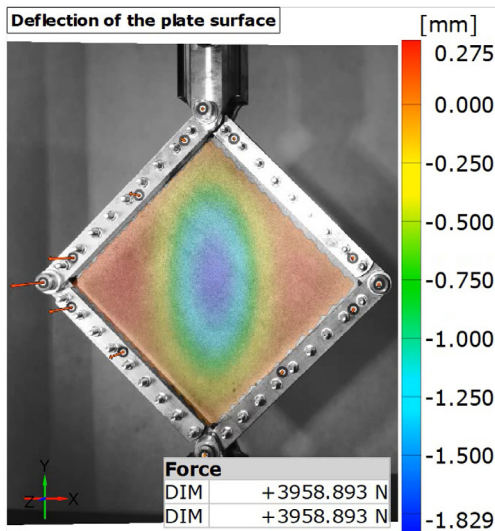


Figure 7. Visualisation of the distribution of displacements in the direction normal to the model plane, for the maximum load value

The load was applied in several successive cycles to eliminate the natural clearances created by the bolted connections. This was the reason for the discrepancy between the characteristics presented. The first relationship (Fig. 8a), corresponding to displacement of the point in the geometrical centre of the plate, shows considerable nonlinearity due to the buckling nature of the deformation. The second relationship (Fig. 8b), on the other hand, has a much smoother, near-linear character, which is due to the relatively small effect of the model's cratered post-critical deformation on its in-plane displacements.

Precise measurements of the displacement distributions of the model cross-sections, corresponding to the main diagonals, were also made (Fig. 9).

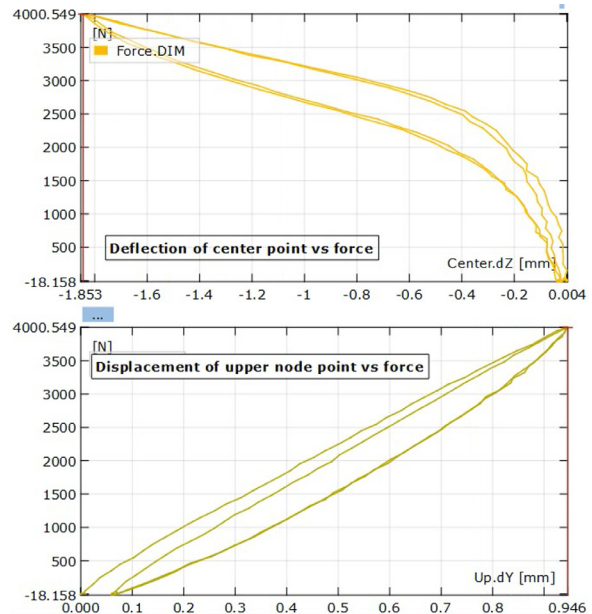


Figure 8. Representative equilibrium paths: (a) the displacement of the centre of the model with respect to its plane in the normal direction, (b) the displacement of the upper joint of the load system in the direction of the load vector

The experimental results provided a reference basis for the numerical solution. To obtain the physical constants needed for the FEA analysis, it was necessary to perform a series of experiments on samples prepared by the incremental technique. Some had a longitudinal and some had a transverse fibre arrangement (Fig. 10). A series of samples with alternate layer orientations, at angles of 45/135 degrees with respect to the sample axis, were also made. The specimen geometry and test conditions were in accordance with ASTM D-638.

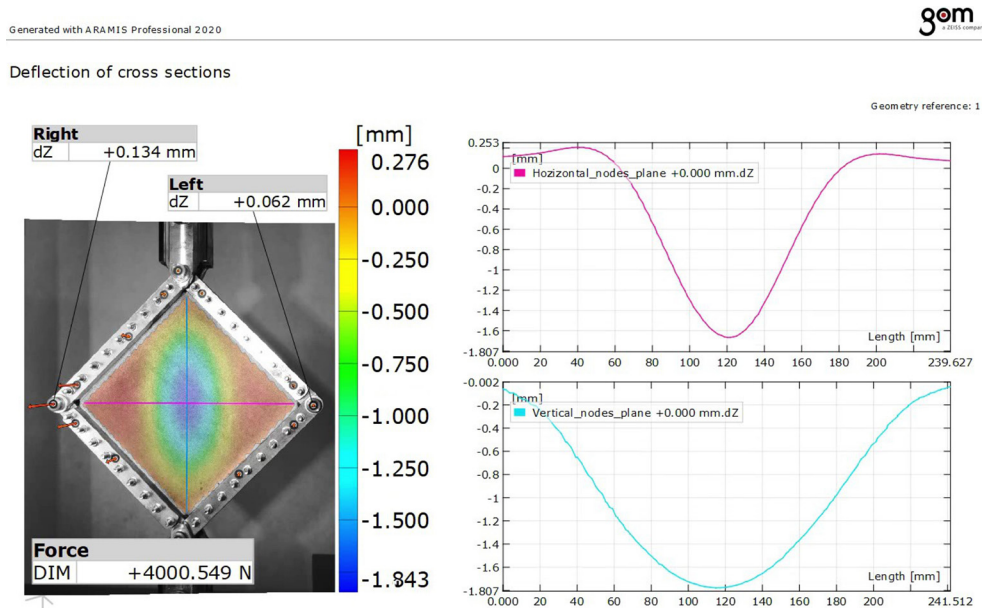


Figure 9. Results of displacement measurements of selected cross-sections of the model at the maximum load value

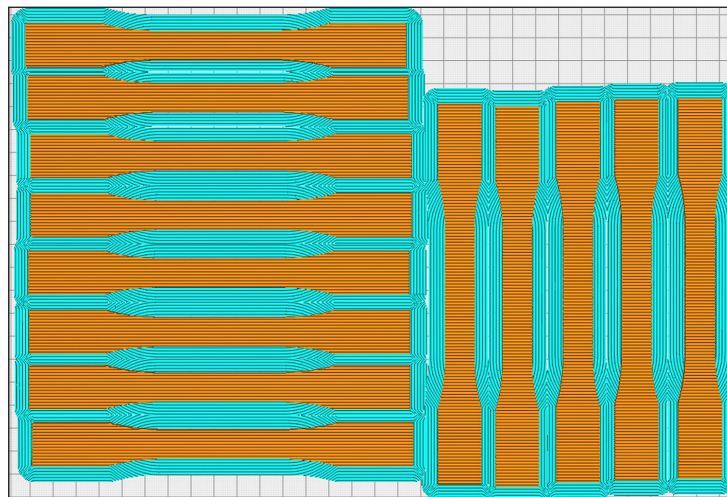


Figure 10. Example visualisation of 3D printed samples for measuring physical constants, using ULTIMAKER CURA software

Experiments have shown that there is a significant difference between the mechanical properties of samples loaded in the direction of the fibre orientation and perpendicular to the fibre orientation, although this difference is much smaller than, for example, in typical fibre composites (Fig. 11–12).

From the properties presented, it can be observed that the reproducibility of the specimen properties was very good when the loads were applied in the printing direction. In contrast, specimens in which the orientation of the strands was perpendicular to the direction of the load vector were characterised by a strong deterioration of the

relationship between normal stress and longitudinal deformation, especially in the higher range of load values. This is because, in the latter case, the cross-sectional weaknesses in the form of fine notches between the paths do not have a perfectly homogeneous character. The geometric form and dimensions of these cavities are the result of the limited accuracy of the space printing process itself. The nonlinearity of the properties at higher stress values is due to the formation of local cohesion loss focal points in the material. It should be noticed that in the lower load areas, which are functionally more important, the reproducibility of the relationships obtained can be considered satisfactory.

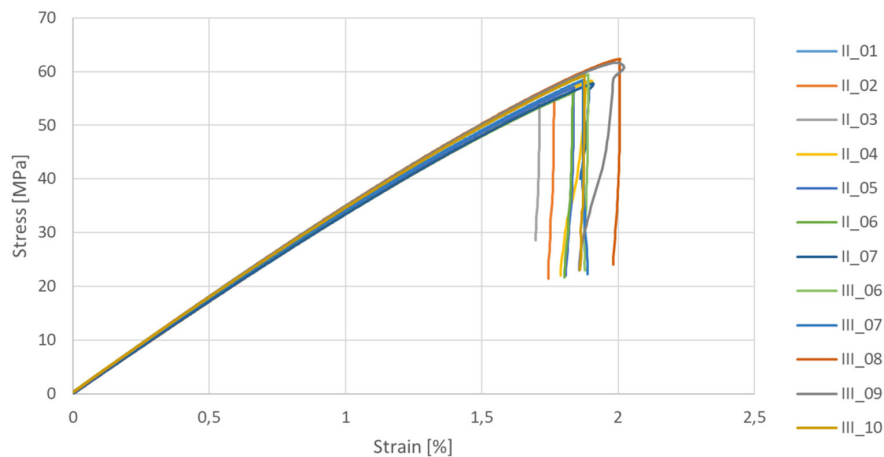


Figure 11. Tensile diagrams of specimens with fibre orientation in the direction of loading

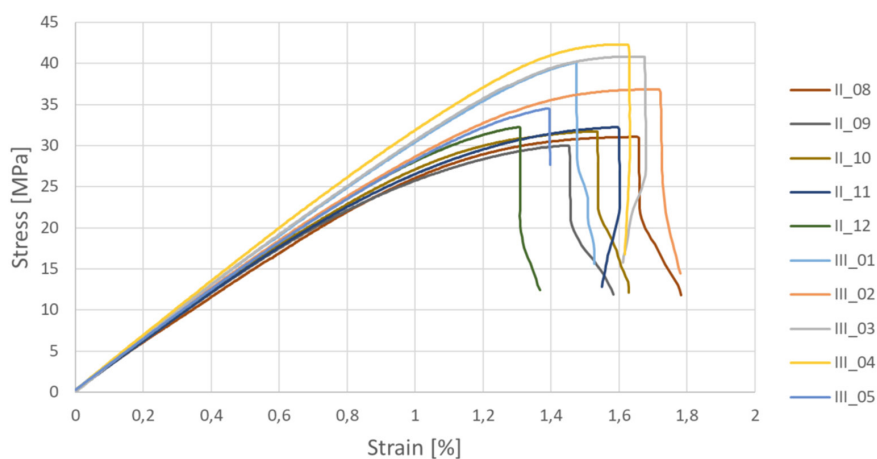


Figure 12. Tensile diagrams of specimens with fibre orientation perpendicular to the direction of loading

To determine the physical constants of the samples from the measured results, one of the typical methods for this type of material was used [6].

The final averaged values of the determined constants were used as the basis for the numerical calculations:

- $E_{11} = 3520\text{GPa}$ – longitudinal modulus of elasticity in the direction consistent with the orientation of the print paths,
- $E_{22} = 3100\text{GPa}$ – longitudinal modulus of elasticity in the direction perpendicular to the print path orientation,
- $G_{12} = 1730\text{GPa}$ – shear modulus,
- $\nu = 0.33$ – Poisson’s ratio.

Numerical analyses

In non-linear numerical analyses, a model with a hybrid structure was used. The structure under test was represented by bilinear thin-shell elements, while the kinematic fixation system was represented by octahedral solid elements.

This created the possibility of a relatively simple mapping of the frame’s articulated joints. Since there were no active rotational degrees of freedom in the solid elements, the kinematic properties of the system (hinges) were mapped using the connections between the contact line nodes of the sharp angles (Fig. 13).

The main problem with numerical analyses of plane-loaded plane models is the inability to represent post-critical deformations. In the real structure, deformations in the direction perpendicular to the plate’s plane are due to natural small geometric and material imperfections. On the other hand, in a numerical model, the geometric structure is idealised, which means that numerical analysis only leads to transitions in the plane of the model. To find a solution that is consistent with the experimental results, it is, therefore, necessary to introduce a forcing that triggers the formation of post-critical deformations or use of the perturbation of linear buckling modes as initial state for analysis [17].

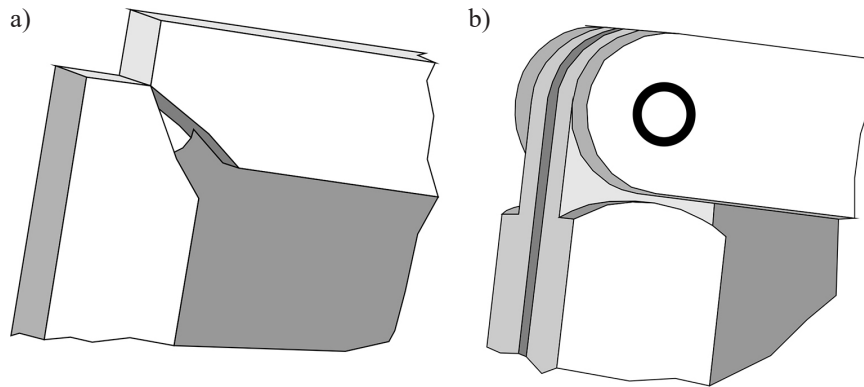


Figure 13. The hinged joint at the corner of the frame: a) model solution, b) actual solution

For the task at hand, a previously developed method [10] was used to apply additional lateral loads at the corners of the model frame (Fig. 14). As a result, the model deflects very little, which does not significantly affect the magnitude of the post-critical deformations, but only allows the equilibrium path of the structure to start branching.

The finite element mesh was created using eight-node solid elements and four-node bilinear thin-walled shell elements. It consisted of a total of 26,279 elements and 39,983 nodes (Fig. 15). However, it should be noted that the majority, 22,608, were solid elements, so the corresponding nodes each had three active degrees of freedom, which had a positive effect on the overall size of the numerical task.

The numerical representation of the structure of the incrementally fabricated structure was based on a model corresponding to a fibre composite (classical lamination theory). Each printed layer corresponds to a model layer whose directional properties are described by the physical constants determined in the experiment. In total, therefore, the model had 20 layers, each 0.1 mm thick.

By using a method in which imperfections were highlighted by small lateral loads, performing a linearised stability analysis was avoided, which is usually used in similar cases to determine the first mode of critical deformation.

In the present case, a nonlinear analysis was used, aiming to determine the equilibrium path of the structure. In the general case, the relationship is a hypersurface in an *n-dimensional* state space, where *n* corresponds to the number of degrees of freedom of the structure. At each step of the analysis, which corresponds to a load increment, the system satisfies the matrix residual force equation [2, 5]:

$$r(u, \lambda) = 0 \tag{1}$$

where: *u* is a state vector containing the displacements of the structure’s nodes corresponding to its current geometric configuration, λ is a control parameter related to the current load level, while *r* is a residual vector containing the unbalanced force components corresponding to the current deformation state of the structure [4, 13, 15].

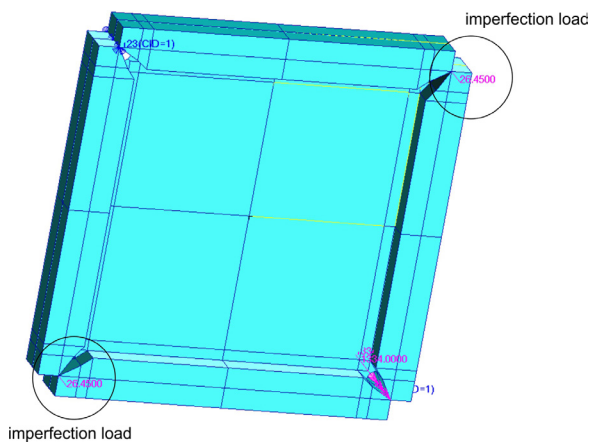


Figure 14. Geometric model with constraints and loads

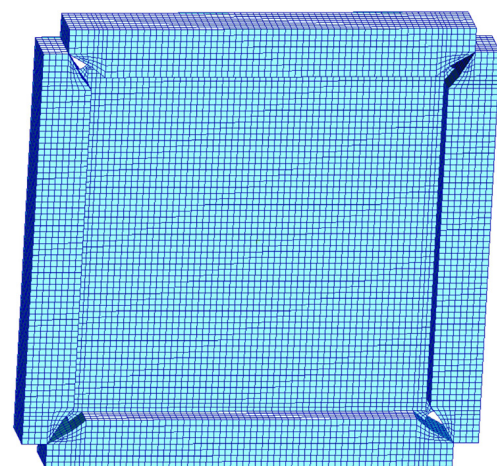


Figure 15. Finite elements mesh

A feature of all nonlinear procedures is the presence of an incremental phase. During each load increment, there is a transition from the n state to the $n+1$ state. The undefined quantities here are increments:

$$\Delta u_n = u_{n+1} - u_n, \Delta \lambda_n = \lambda_{n+1} - \lambda_n, \quad (2)$$

Their determination requires the formulation of an additional equation, called the incremental control equation, or constrains equation:

$$c(\Delta u_n, \Delta \lambda_n) = 0 \quad (3)$$

It represents a user-defined state resulting from an approved correction strategy.

The different types of commercial software allow the user to choose different degrees of incremental methods and correction strategies. In the case of MSC MARC, it is possible that the parameters driving the nonlinear procedures are subject to a relatively large amount of interference.

In the case described here, the Newton-Raphson incremental method was used, combined with a load control (state correction) strategy [15].

The analysis resulted in the deformation distribution of the model (Fig. 16).

To compare the deformations obtained by nonlinear numerical analysis with the results of experiment, the components of the deformed mesh were isolated from regions corresponding to the main diagonals of the structure, i.e. the cross-sections indicated in Fig. 9. After appropriate scaling of the resulting outlines, a comparison was made with the experimental results (Fig. 17).

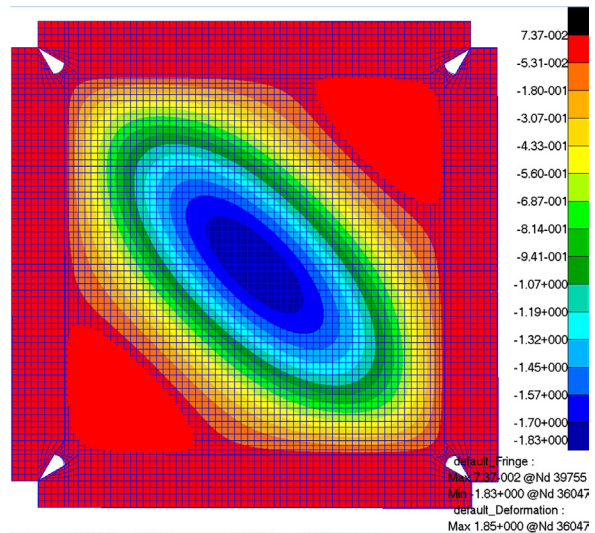


Figure 16. Distribution of displacements in the direction normal to the model plane, compared with the undeformed mesh

The comparison presented here shows that the deformations are remarkably similar both qualitatively and quantitatively.

The overall shape of the numerically obtained transition field and its minor deviations from the experimentally determined distribution are largely due to the finite element mesh concept. Its regular shape resulted from the desire to precisely target the physical properties of the individual composite layers. These properties are defined by the software user relative to the global reference coordinates. It is therefore important to achieve

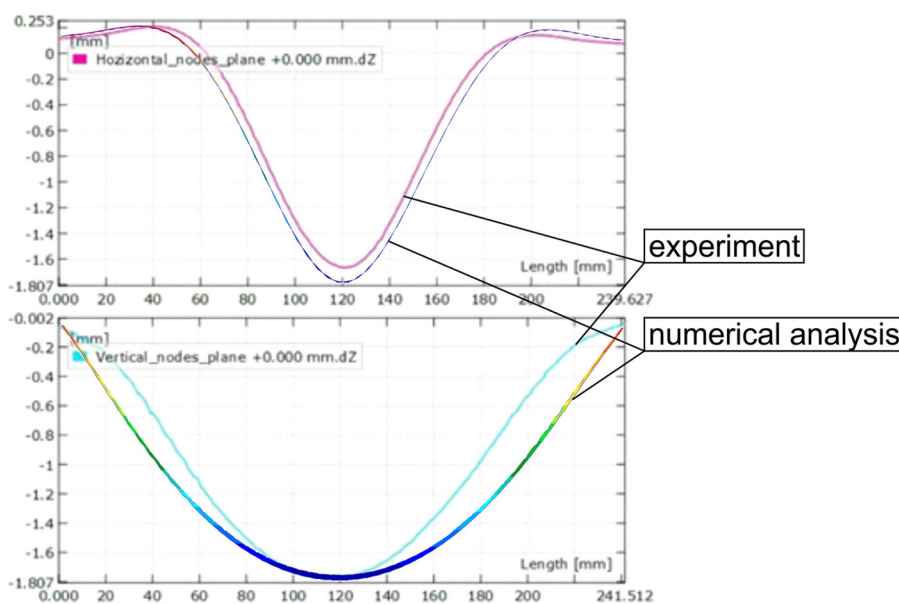


Figure 17. Summary of the distribution of displacements in the direction perpendicular to the plane of the model for selected cross-sections corresponding to the main diagonals of the structure

consistency in the orientation of the global system axes and the local system axes of the individual elements.

The differences between the deformation distributions corresponding to the selected characteristic sections are due to the simplified boundary conditions used in the numerical model. The connection between the nodes of the shell elements and the nodes of the solid elements is articulated because, as already noted, the rotational degrees of freedom are not active in the solids. This affects the value of the tangent angles to the distributions shown above at the points corresponding to the zero displacement values.

During the study, numerical testing of the model was also carried out, in which an additional layer of shell elements was mapped between two layers of solid elements, corresponding to the fixing of the edges of the model under study between the frame elements. However, this solution led to excessive structure stiffness due to incorrect numerical considerations [16, 17, 18]. In addition, in a real structure, the stiffness of the model is affected by bolted connections, which do not seem appropriate to be represented in a model based partly on solid elements. This would require a very high-density mesh grid or elements of very different sizes.

CONCLUSIONS

The presented variant of the numerical representation of the structure that is the subject of the experiment is one of a number of possible solutions. From the point of view of its purpose for nonlinear analysis, its relatively simple structure seems to be an advantage, allowing a satisfactorily correct solution to be obtained without the need for contact functions and *multi-point constraint* connections. Although the lateral deformations obtained by the numerical and experimental methods do not fully match, from a technical point of view, the correct representation of the stiffness of the shell model, which allows the maximum values of the post-critical displacements to be determined, seems to be the most important. Given that these discrepancies are relatively small, the result of the nonlinear numerical analysis can be considered satisfactory. Therefore, the use of the described hybrid model, based on solid and surface elements, allows for results that are useful in design processes.

From this it can be concluded that the mechanical properties of the structure are correctly represented using the concept of a layered fibre composite model. The method used to determine the physical constants of the incremental compression structure by experimentally testing samples with a two-way extensometer also appears to be effective. It seems necessary to determine the above constants for a given filament since there can be considerable differences in the mechanical properties of different filament types.

The considerations presented allow further research directions to be identified. The versatile nature of the test bench and the considerable scope for modifying structures using incremental techniques allow experiments to be carried out on geometrically diverse models. The concept of analysing models with integral reinforcements seems particularly interesting.

At the same time, the experimental results can provide reference material for the development of new solutions for the numerical representation of the above structures.

REFERENCES

1. Arborecz J. Post-buckling behavior of structures. Numerical techniques for more complicated structures. Lecture Notes In Physics. 1985; 288: 83–142.
2. de Borst R., Crisfield M.A, Remmers J.J, Verhoose C.V. Non-linear finite element analysis of solid and structures. Second edition, J. Wiley & Sons, Hoboken, New Jersey, USA 2012.
3. Dębski H., Sadowski T. Modelling of microcracks initiation and evolution along interfaces of the WC/Co composite by the finite element method. Computational Materials Science 2014; 83, 403–411.
4. Doyle J.F. Nonlinear analysis of thin-walled structures, Springer-Verlag, Luxemburg 2001.
5. Felippa C.A., Crivelli L.A., Haugen B. A survey of the core-congruential formulation for nonlinear finite element, Archives of Computer Methods in Engineering 1994; 1, 1–48.
6. Ferreira A.J.M., Amate I.C., Dutra T.A., Bürger D., Experimental characterization and micrography of 3D printed PLA and PLA reinforced with short carbon fibers, Composites Part B: Engineering 2017; 124: 88–100.
7. Hanon M., Dobosa J., Zsidaia L. The influence of 3D printing process parameters on the mechanical performance of PLA polymer and its correlation with hardness, Procedia Manufacturing 2021; 54: 224–229.

8. Kopecki T., Bakunowicz J., Lis T. Post-critical deformation states of composite thin-walled aircraft load-bearing structures, *Journal of Theoretical and Applied Mechanics* 2016; 54(1): 195–204.
9. Kopecki T. Numerical-experimental analysis of the post-buckling state of a multi-segment multi-member thin-walled structure subjected to torsion. *Journal of theoretical and applied mechanics* 2011; 49(1): 227–242.
10. Kopecki T. Selected Methods of Obtaining Adequate Forms of Deformation of Supercritical Thin-Walled Flat Plates, *Advances in Science and Technology Research Journal*. 2021; 15(2): 184–190.
11. Kratochvíl J., Sadilek M., Musil V., Stančková D. The effectiveness of strategies printing printer easy 3D maker, *Advances in Science and Technology Research Journal*. 2018, 12(2): 197–205.
12. Lynch C.A. Finite element study of the post buckling behavior of a typical aircraft fuselage panel, PhD Thesis, Queen's University Belfast, UK 2000.
13. Mazurek P., Fatigue Strength of Thin-Walled Rectangular Elements in the State of Post-Critical Deformation, *Advances in Science and Technology Research Journal*. 2019; 13(2): 84–91.
14. Monaldo E., Ricci M., Marfia S. Mechanical properties of 3D printed polylactic acid elements: Experimental and numerical insights, *Mechanics of Materials*. 2023; 177: 104551.
15. Riks E. An incremental approach to the solution of snapping and buckling problems. *International Journal of Solid and Structures* 1979; 15, 529–551.
16. Różyło P., Dębski H., Kral J., Buckling and Limit States of Composite Profiles with Top-Hat Channel Section Subjected to Axial Compression, *Conference: 22nd International Conference on Computer Methods in Mechanics (CMM)* Location: Lublin Univ Technol, Lublin, POLAND SEP 13-16, 2017.
17. Świąch Ł. Experimental and Numerical Studies of Low-Profile, Triangular Grid-Stiffened Plates Subjected to Shear Load in the Post-Critical States of Deformation, *Materials* 2019; 12: 3699.
18. Świąch Ł. Experimental and numerical analysis of the post-buckling behaviour of integrally sub-stiffened rectangular plates subjected to shear, Pietraszkiewicz, W., & Gorski, J. (Eds.). (2013). *Shell Structures: Theory and Applications: Volume 3* (1st ed.). CRC Press.
19. Tirado-Garcia I., Garcia-Gonzalez D., Garzon-Hernandez S., Rusinek A., Robles G., Martinez-Tarifa J.M.e, Arias A. Conductive 3D printed PLA composites: On the interplay of mechanical, electrical and thermal behaviours, *Composite structures* 2021; 265: 113744.
20. Torre R., Brischetto S., Rocco Dipietro I. Buckling developed in 3D printed PLA cuboidal samples under compression: Analytical, numerical and experimental investigations, *Additive Manufacturing* 2021; 38: 101790.